 doi:10.20944/preprints202103.0604.v1

*Short Note*

# *N,N*-bis(2-quinolinylmethyl)benzylamine.

**Leigh A. Hunter [1], Shivani Naidoo[1] and Allen Mambanda[1,*]**

[1]School of Chemistry and Physics, University of KwaZulu-Natal, Private Bag X01, Scottsville, Pietermaritzburg, 3209, South Africa.;
HunterL@ukzn.ac.za; "shivanin.21@gmail.com; mambanda@ukzn.ac.za
*Correspondence: mambanda@ukzn.ac.za; https://orcid.org/0000-0002-8113-3643

**Abstract:** The compound, $C_{27}H_{23}N_3$ (**1**), crystallizes in the triclinic system of the *P-1* space group. The unit cell comprises a dimer of **1**, in which the monomers are linked by two complementary hydrogen bonds between N1 and H′1-C′1 of another molecule. The dimers form chains along the *a*-axis through intermolecular interactions between the N′2 acceptor atoms and C′′17 donors from molecules in the nearest neighbouring dimer. These interactions form extended sheets of the dimers of **1**, along the *ab* plane. The quinolinylmeth-2-yl groups of **1** lie in almost orthogonal planes and their $N1/2_{(q)}$ donor atoms being away from the apical amino N3 atom.

**Keywords:** H-bonds (-bonding): hydrogen bonds (-bonding); q: quinoline; 3-/2D: three-/two dimensional & VdW: Van der Waal & bqma: bis(2-quinolinylmethyl)amine

## 1. Introduction

Bis(2-pyridinylmethyl)amines (bpmas) (**I**) and their closely related analogues, bis(2-quinolinylmethyl)amines (bqmas) (**II**) are versatile N^N^N tridentate ligands that form mononuclear metal complexes with flexible five-membered chelates [1-7]. *Bis*(2-quinolinylmethyl)benzylamine (**1**), a derivative of the bqma ligands with an appended benzyl group at the amine position was first reported by Kryatov *et al*. [1]. However, its crystal structure has not been reported to date. In that report of Kryatov *et al*. [1], **1** was used together with other iso-structural ligands for stabilizing dinuclear complexes with a common Fe(II)(μ-OH)$_2$ core. Soon after, Kunishita *et al*. [2] used this ligand for the synthesis of Cu(II) complexes. More recently, Li *et al*. [5] have synthesized monomeric Ni(II) and Cu(II) complexes of **1** and studied their binding affinity to CT-DNA and bovine serum albumin (BSA) to infer their potential as anticancer therapeutics.

There are no literature reports on *d8*-square-planar coordination complexes of **1** or its bqma derivatives other than one recently reported for Pt(II) complexes supported by the structurally related ligands, benzyldi(2-pyridyl)amines [6]. The latter complexes demonstrated that benzylation of ligands afforded tuneable conformational flexibility to the resultant complexes and the same structural effect could be applied for square-planar complexes of benzylated bqma/bpma ligands. Also imposed on one of the faces of the aforementioned Pt(II) complexes was a significant aerial steric effect due to the near orthogonal orientation of the benzyl group on one side of the square-plane of the complexes. Mikita *et al*. [7-10] have fabricated Zn(II)/Cd(II) off/on-fluorescence sensors using the bqma-derived hexadentates, linked by 1,2-ethylenediamine [6] and lately by 1,2-phenyl-/cyclohexyldiamines [7,8]. They have reported also the crystal structure of *tris*-(isoquinolinemeth-1-yl)amine [10], an analogue of **1** which has an iso-structural N^N^N tridentate head group and a closely related isoquinolinemeth-1-yl as a pendant group at the amine position. We have previously synthesized type-**I** [11-12] and lately hemi-type-**II**-based N^N^N tridentates (whose structures are shown in Figure 1) for coordinating Pt/Pd(II) ions. Complexes were used for studying trends in the rates of substitution of labile co-ligands.

Preprints (www.preprints.org) | NOT PEER-REVIEWED | Posted: 24 March 2021 doi:10.20944/preprints202103.0604.v1

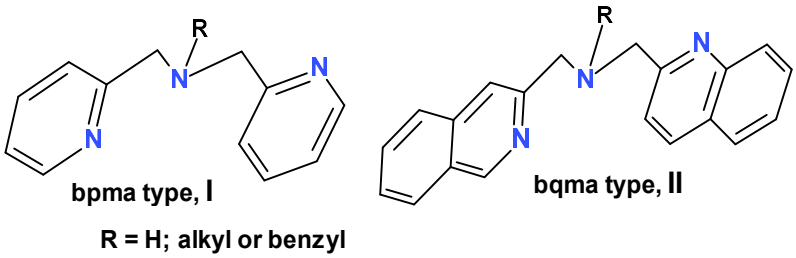


**Figure 1**. Structures of the *bis*(2-pyridinylmethyl)amine (bpma)s (type-**I**) and *bis*(2-quinolinylmethyl)amine (bqma) (type-**II**) ligands.

## 2. Results

The search for tridentate N-donor ligands for coordinating to Pt/Pd(II) ions has led us to explore the synthesis of **1**, whose crystal structure was solved by single-crystal X-ray diffraction analysis. Crystal data of **1** and structure refinement details are summarised in Table 1. The ORTEP representation of the asymmetric unit with the atoms numbering scheme is shown in Figure 2. Selected bond lengths and angles are presented in the caption of the Figure.

**Table 1.** Crystal data and structure refinement for **1**.

| Identification code for 1 | l1_sq |
|---|---|
| Empirical formula | $C_{27}H_{23}N_3$ |
| Formula weight | 389.48 |
| Temperature | 100(2) K |
| Wavelength | 0.71073 Å |
| Crystal system | Triclinic |
| Space group | P -1 |
| Unit cell dimensions | a = 8.7296(6) Å, α= 70.914(2)°. |
| | b = 11.1447(6) Å, β= 86.955(2)°. |
| | c = 12.3411(6) Å, γ = 74.653(2)°. |
| Volume | 1093.45(11) $Å^3$ |
| Z | 2 |
| Density (calculated) | 1.183 $Mg/m^3$ |
| Absorption coefficient | 0.070 $mm^{-1}$ |
| F(000) | 412 |

Preprints (www.preprints.org) | NOT PEER-REVIEWED | Posted: 24 March 2021 doi:10.20944/preprints202103.0604.v1

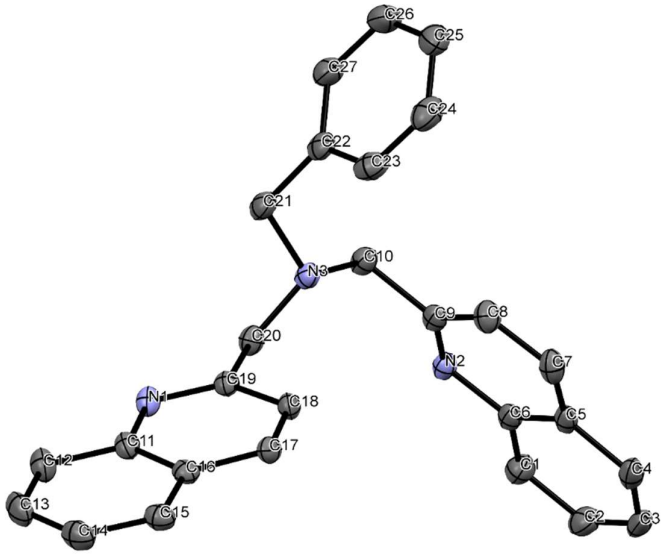


**Figure 2.** ORTEP drawings of the asymmetric unit of **1**. Thermal ellipsoids are drawn at the 50% probability level. Selected bond lengths (Å) and angles (°) are: N(1)-C(19) 1.3165(16); N(1)-C(11) 1.3772(17); N(2)-C(9) 1.3151(17); N(2)-C(6) 1.3768(16);C(20)-N(3)-C(21) 112.04(10); C(20)-N(3)-C(10) 111.57(10) & C(21)-N(3)-C(10) 112.74(10).

### 3. Discussion

Compound **1** crystallizes in the triclinic system of the *P-1* space group. The unit cell comprises two molecules of **1** linked by two complementary hydrogen bonds to form an inversion dimer. The monomers are linked by two complementary hydrogen bonds between the $N1_{(q)}$ atom (the hydrogen bond acceptor, *q* = quinoline ring) and the C′1H′1 (hydrogen bond donor) on the benzo ring of the quinoline ring of an adjacent molecule of **1** to form a cyclic supramolecular motif in the *ab* plane as shown in Figure 3. The H′1 atom is at a distance of 2.732 Å from the $N1_{(q)}$ atom of its dimer partner. This bond distance is significantly shorter than the sum of the Van der Waals (VdW) radii of the interacting nuclei but is not quite linear (with an ∠*C1-H1…N1* of about 151.30°, see Table 2) as would be expected for an ideal dipolar H-bond. Inclusive of the two complementary hydrogen-bonds, the loosely-held and puckered supramolecular cyclic motif of the dimer comprises 22 bonds, whose monomers are related by an imposed centre of inversion. Similar structural packing in the solid, stabilized by dimeric conformations in the solid-state has been reported for structurally related compounds [6, 13-14]

Preprints (www.preprints.org) | NOT PEER-REVIEWED | Posted: 24 March 2021 doi:10.20944/preprints202103.0604.v1

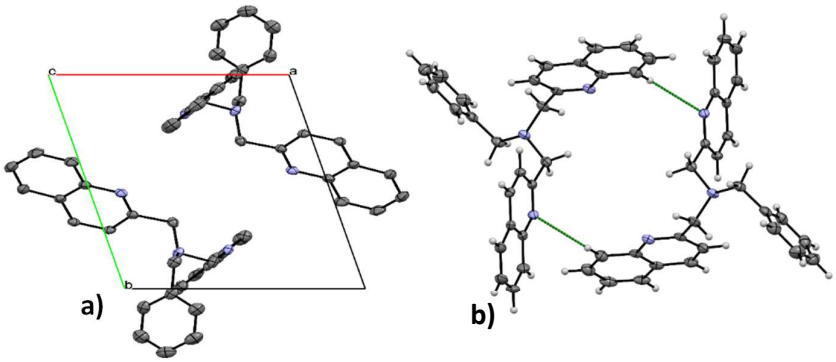


**Figure 3**. The partially filled *P-1* unit cell of **1** (viewed along the *c*-axis), showing the dimeric structure of **1,** supported by two complementary hydrogen bonding interactions (represented by dashed lines).

The dimers form linear chains along the *a*-axis through another set of [CH….N] hydrogen bond contacts [d(*H*—*A*), Å = 2.749], occurring between the N″2(*q*″) acceptor atoms from molecules in the nearest neighbouring dimer and the H′17′ donor atoms (refer to Figure 4 for a perspective view). These interactions are also complementary and lie in a plane that is nearly orthogonal to the former set of contacts, and link up the discrete dimers of **1** into extended sheets along the *ab* plane. In these chains, the quinolyl rings bearing the N2 atoms of each dimer partner are involved in endogenic but seemingly weak slip-up $\pi$-$\pi$ interactions in the interior of the stacking network while the exteriors are flanked by the benzyl pendants of each dimer partner. The sheets are in turn cross-linked by other non-classical short contacts, thus forming an infinite, three-dimensional supramolecular structure. Although hydrogen bond length does not necessarily correlate linearly to bond strength, due to packing constraints in the lattice, these bonds are considerably shorter than the sum of their van der Waals radii and are thus likely to be moderate to high in strength. This also seems likely to be the case of the solid structure of **1** as the D—H···A bond angle of both bonds, 151.30 (1)° and 147.19 (1)° for N1···H′1—C′1 and N2···H′17—C′17, respectively, do not show a marked deviation from the ideal linear angle. The key intermolecular hydrogen bond lengths and angles in the solid structure of **1** are summarized in Table 2.

**Table 2**. Key intermolecular hydrogen bonds lengths and angles in the solid structure of **1**

| *D* | *H* | *A* | d(*D*—*H*), Å | d(*H*—*A*), Å | d(*D*—*A*), Å | ∠*D*—*H*…*A*,° |
|---|---|---|---|---|---|---|
| C′17 | H′17 | N2 | 0.950 | 2.732 | 3.594(2) | 151.30 |
| C′1 | H′1 | N1 | 0.950 | 2.749 | 3.584(2) | 147.19 |

Preprints (www.preprints.org) | NOT PEER-REVIEWED | Posted: 24 March 2021 doi:10.20944/preprints202103.0604.v1

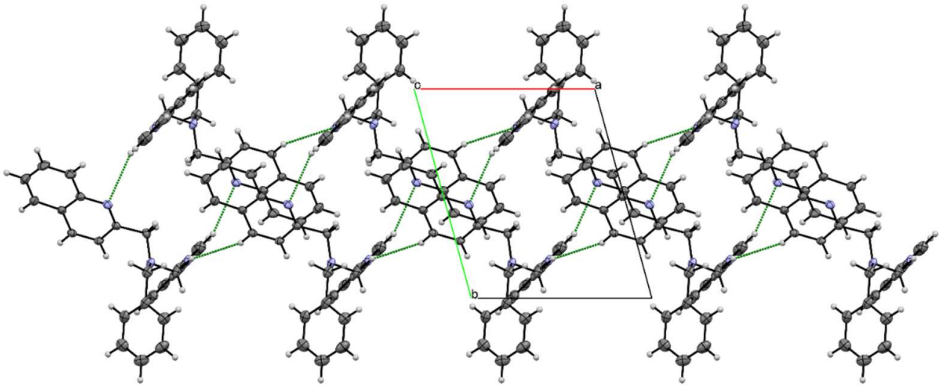


**Figure 4**. A view along the *c*-axis showing the 1D-hydrogen bonded column of dimers of **1** (projecting along the *ab*-plane).

The complementary hydrogen interactions which link up two molecules of **1** in the dimers may help to stabilize the dimer lattice, given the possible weak intermolecular forces between monomer pairs of **1** due to their marked asymmetry. The described H-bonds enable columnar stacks of centrosymmetric dimers of **1** along the *a*-axis. The presence of significantly large voids in the dimeric lattice of **1** reflects the loose packing in its 3D structure due to the bulkiness of the three methylene bridged groups around the amine bridgehead (N3). The voids seem large enough to accommodate molecules of the crystallization solvent (ethanol), refer to Figure SI 1 (ESI) for an illustrative view.

As shown in the structure of the asymmetric unit (Figure 2 or 5), the three bridging methylene groups adopt a non-staggered conformation and are located on the basal plane of the trigonal pyramidal about the amine N3 atom. This conformation is similar to what has been reported for the molecular structure of the *tris*-(isoquinolinemeth-1-yl)amine[10], an analogue of **1** which has an iso-structural bqma head group.

The conformation of the three groups about the apical N3 places all methylene groups in the vicinity of the trigonal pyramid's edges with a *syn-syn-syn* orientation about the basal plane. The amine N3—$C_{(methylene\ bridgeheads)}$ bond distances are typical and lie in the range 1.4633(18)-1.4669(17) Å. The lone pairs of electrons on the $N3_{(amine)}$ atom also repel the bridgehead methylene hydrogens in equal forces in space, making angles (∠C'N3C'') about the $N3_{(sp^3\ hybridized)}$ in the range 109.88(11)°-112.74(11)°. This ensures the least-energy conformation of **1**. The conformation geometry about the amine is quite similar to that reported for the structurally related analogues, *viz.* tris-2-(quinolinylmethyl)anime [10] and some benzyldi(2-pyridyl)amine derivatives [6]. Thus, the steric influence of the benzyl group on the 2-quinolinylmethyl arms of the N^N^N head group of the free ligand (**1**) is minimal. However, its orthogonal disposition of the pendant group is likely to have a measurable steric induced effect on one side of the square-planar metal complexes of ligand **1**, as highlighted in the conformational flexibility of Pt(II) complexes stabilized by the benzyldi(2-pyridyl)amine [6] ligand bearing substituents of varying degree of steric influence on the benzyl pendant. Also, the quinolinylmeth-2-yl groups which are located at the two of the edges of the trigonal pyramid which has the amine N3 as its apical atom, lie in almost orthogonal planes (least square mean plane-to-plane angle between their rings of 110.4°) and are in an *anti, anti* orientation to the $N3_{(amine)}$ atom, refer to Figure 5 for a

Preprints (www.preprints.org) | NOT PEER-REVIEWED | Posted: 24 March 2021 doi:10.20944/preprints202103.0604.v1

perspective view. This minimizes mutual lone-pair/lone-pair electron repulsions in space between the lone pairs of the N1/N2$_{(q)}$ atoms of the quinolinyl groups. Noticeably, the three nitrogen atoms N1/N3/N2 are not suitability orientated for N^N^N chelation (pincer-type) with $d^8$ metal ions. For this to happen, there has to be a rotation about the C9—C10 and C19—C20 bonds. The near-orthogonal orientation and relative flexibility of the quinolinylmeth-2-yl groups also allow for the afore-described non-conventional hydrogen bonding which seems to stabilize the lattice of **1** in the solid as already discussed (*vide supra*).

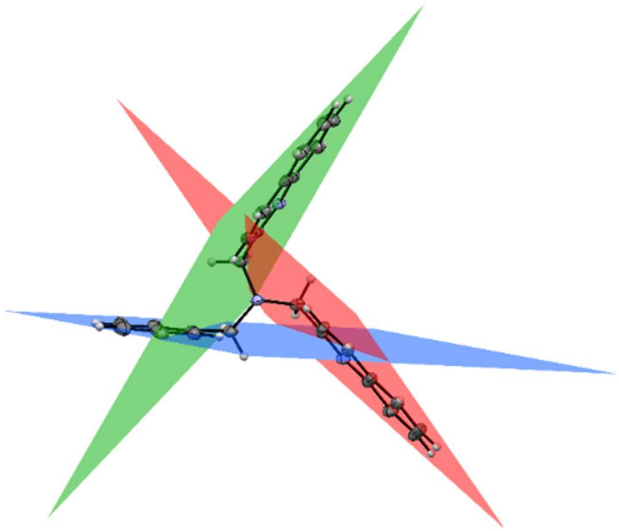

Figure 5. Disposition of the methylene bridged groups about the amine nitrogen (N3), showing a marked asymmetry in the structure of **1**.

To further understand the dimeric structure of **1**, DFT (using the B3LYP/6-311G(d,p)* basis set [15-17]) optimized structures of **1** and its hydrogen-bonded dimer were simulated in the gaseous state using Gaussian 9 [18] suite of programs, starting from the coordinates of the solved crystal structure of **1**. The simulated structure of **1** is presented as an overlay of the crystal structure in Figure 6a. The DFT optimized structures of the dimer, the frontier molecular orbitals and the energy-band diagram are presented in Figure 6b and Figure SI 2 (ESI), respectively.

Preprints (www.preprints.org) | NOT PEER-REVIEWED | Posted: 24 March 2021 doi:10.20944/preprints202103.0604.v1

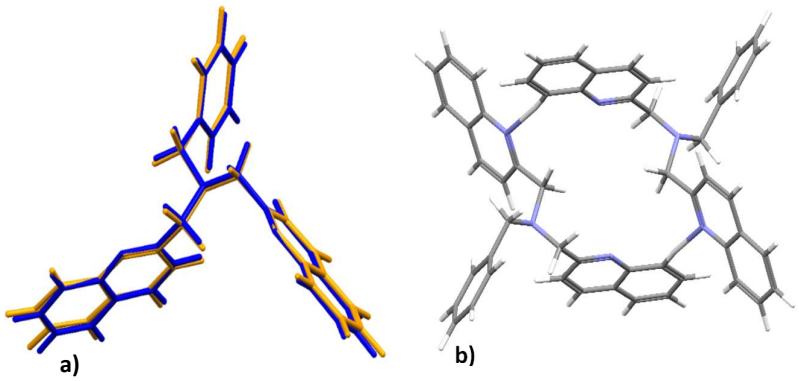


**Figure 6. a)** Superimposed structures of the X-ray crystal structure of **1** (blue) and DFT optimized structure (orange), showing a near-perfect fit of the latter to the crystal structure with a mean square root deviation (for all non-hydrogen atoms) RMSD (Å) of 0.1525). **b)** DFT optimized structures of the dimer of **1**, formed through complementary [N1….H′1C′1] hydrogen bond contacts.

As depicted in Figure 6a, there is a near-perfect fit between the simulated structure of **1** and the X-ray crystal structure with an RMSD of 0.1525Å. The low RMSD is an indication that the level of theory used to perform the simulative calculations is reliable in predicting the geometric structures of both the monomer and its dimer as well as the energetics of their frontier orbitals in the gaseous state. However, and as shown in Figure SI 1 (ESI), there seems to be no significant difference in the energies of the HOMO/LUMOs and the energy bandgap for the dimer and **1**. Thus, the calculated data did not suggest the dimeric structure of **1** (as depicted in Figure 6b) in its supramolecular structure is driven by the need to minimize its internal energy states, at least in the gaseous phase.

## 4. Materials and Methods

*4.1. Synthesis of bis(2-quinolinylmethyl)benzylamine* (**1**)

Compound **1** was synthesized by the method of Kryatov *et. al.*[1] with some minor modifications. Under an inert atmosphere of flowing nitrogen, benzylamine (0.17 mL, 1.5 mmol) was added (in drops) to a stirred alkaline solution (pH > 9) of a solution of 2-quinolinylmethyl chloride hydrochloride (0.5 g, 3.0 mmol) dissolved in 1.5 mL of 5.0 M KOH and catalytic amounts of *tert*-butylammonium tetrachloride. The mixture was stirred at 50 °C for 3 days. Thereafter, about 1 g of NaCl was added and the mixture was extracted with 3x10 mL portions of chloroform and acetonitrile (9:1). The combined organic extracts were back-washed with 3 x 5 mL aliquots of ultrapure water. The organic layer was dried over $MgSO_4$, filtered and the filtrate was concentrated before it was chromatographed on neutral alumina (ca. 2 g) using a 9:1 mixture of chloroform and methanol. The collected light yellow extract was concentrated, yielding a yellow-orange oil. The dried oil was layered with dry ethanol and allowed to evaporate slowly. Colourless crystal blocks of **1** suitable for single X-ray diffraction analysis were yielded after two days.

Preprints (www.preprints.org) | NOT PEER-REVIEWED | Posted: 24 March 2021 doi:10.20944/preprints202103.0604.v1

*4.2. Spectroscopic characterization of* **1**

Compound **1** was characterized by several spectroscopic techniques. NMR spectra were acquired on a Bruker-AVANCE III 400 MHz NMR spectrometer with an AA 9.4 Tesla magnet and a 5 mm BBO sample probe, using $CDCl_3$ as a solvent. Mass spectral data was acquired by direct injection of a solution of **1** (in acetonitrile modified with 0.1% formic/formate buffer) into a Waters Micromass LCT Premier MS instrument equipped with an electrospray ionization ($ESI^+$) source and a time-of-flight (TOF) mass analyzer. Elemental analysis was carried out using a CHNS-O Flash 2000 Organic Elemental Analyser. The infrared spectrum was recorded using a Bruker Alpha FTIR spectrometer equipped with an ATR platinum Diamond 1 reflectance accessory. The UV-Visible absorption spectrum was acquired on a Perkin Elmer Spectrum 25 spectrophotometer. *Yield*: 577 mg (92%), low melting point colourless crystal blocks. $^1H$ δ ppm ($CDCl_3$, 400 MHz;): 3.80 (s 1H); 4.15 (s, 1H); 7.25 (t, 4H); 7.49 (d, 2H); 7.69 (t, 2H); 7.79 (d, 2H); 8.06 (d, 2H); 8.08 (d, 2H). $^{13}C$ δ ppm (107 MHz; $CDCl_3$): aromatic: 130; 129; 128; 127; 126; 121; 77 ($CH_2$ - arms).

Elementary analysis: *Calculated for* $C_{27}H_{23}N_3$, %C, 83.26; %H, 5.95; %N, 10.79; *found*, %C, 83.09; %H, 5.87; %N, 10.16. MS-$ESI^+$: *calc. for* $M^+$ for $[C_{27}H_{23}N_3+H]^+$ = 390.1892; found, 390.4799 (100%, $[M+H]^+$), 242.2847 (80%, [M less the (2-quinolinylmethyl $CH_2$ -arms)+H]$^+$

FTIR[1] $cm^{-1}$ (*strong(s)/medium(m)/weak(w)*: 427 (*w*), 475 (*w*), 618 (*m*), 738 (*vs*), 764 (*vs*), 789(*s*), 961(m), 987 (*m*), 1120 (*m*), 1244 (*m*), 1308 (*w*), 1424(*m*), 1502(*m*), 1601 (*m*).

UV-Visible absorption ($CHCl_3$), λ, nm (ε, $M^{-1}$ $cm^{-1}$, peak shape): 268 (~ $1.1x10^3$, shoulder); 319 (~ $4.5x10^3$, broad).

*4.3 X-ray diffraction*

Single crystal X-ray crystallographic data of **1** were collected on a Bruker APEX Duo [19] CCD area detector diffractometer with an Incoatec microsource operating at 30 W of power. The crystal was kept at 100.15 K during data collection using an Oxford Instruments Cryojet accessory. Diffraction was by graphite-monochromated Mo $K_\alpha$ radiation ($\lambda$ = 0.70073 Å (2.0 kW), at a crystal-to-detector distance of 50 mm. Data collection was done at the following set conditions: ω-/ϕ-scans with exposures taken at 30 W X-ray power and 0.50 frame widths using SAINTS' APEX2 [20]. The crystal structure was solved with Olex2 [21], while the SHELXS [22] and SHELX [23] programs were used for structural refinement via direct methods. The non-hydrogen atoms were refined anisotropically by full-matrix least-squares minimization/refinement of $F^2$. Hydrogen atoms were included but not refined. Visualization of the crystallographic data was done in WinGX [24] and Mercury *v.4*.3 [25.]

*4.4 DFT optimized structures*

Starting from the X-ray geometric coordinates, **1** and its hydrogen-bonded dimer were computationally optimized for their low-energy confirmations at the DFT level of theory using the B3LYP/6-311G(d,p) [15-17] method. These calculations were run on GAUSSIAN 09W [17]. The data of the optimized structures were analyzed to further understand the supramolecular structure of the **1** in the crystalline solid-state.

## 5. Conclusions

Compound **1** was synthesized via a double nucleophilic substitution of benzylamine by 2-quinolinylmethyl)chloride hydrochloride under basic conditions. It was characterized by IR, $^{1}$H NMR, $^{13}$C NMR, mass spectrometric methods, elemental analyses and its molecular structure solved by single x-ray diffraction analysis. It crystallizes in the triclinic system of the *P-1* space group. The unit of the cell comprises two molecules of **1** linked by two complementary hydrogen bonds to form an inversion dimer. The dimers of **1** are linked by two complementary hydrogen bonds between N1 and H′1-C′1 of another molecule. The dimers form chains along the *a*-axis through intermolecular interactions between the N′2 acceptor atoms and C′′17 donors from molecules in the nearest neighbouring dimer. These interactions form extended sheets of the discrete dimers of **1** along the *ab* plane. The quinolinylmeth-2-yl groups of **1** lie in almost orthogonal planes with their N1/2$_{(q)}$ donor atoms being away from the apical amino N3 atom.

**Supplementary Materials:** The following data is available online at www.mdpi.com/xxx/s1: Figure S1 1: The linear chains of the dimers of **1**, showing the exogenous voids that can include solvent molecules; Figure SI 2: The DFT HOMO-LUMO energy-band diagram for **1**; Table SI 1: Atomic co-ordinates ( x $10^4$) and equivalent isotropic displacement parameters (Å$^2$x $10^3$) for **l**1_sq; Table SI 2: Bond lengths [Å] and angles [°] for l1_sq (**1**).

**Author Contributions:** ***LH***: X-ray diffraction data collection, data visualization, analysis theoretical calculations; ***SN***: Investigation, Methodology, drafting; ***AM*****:** conceptualization, supervision, data analysis, drafting and review, resourcing.

**Funding:** This research received no external funding.

**Data Availability Statement:** Crystallographic data for the structural analysis of **1** and other illustrative Figures accompany this report as Supplementary information (SI).

**Acknowledgments:** This work was supported by laboratory infrastructure in the School of Chemistry and Physics, PMB Campus, University of KwaZulu-Natal, RSA.

**Conflicts of Interest:** No potential conflict of interests or competing interests is foreseen

## References

1. Kryatov, S. V. et al. Dioxygen binding to complexes with $Fe^{II}_2(\mu\text{-}OH)_2$ cores: Steric control of activation barrier and O2-adduct formation. *Inorg. Chem*. **2005**, *44*, 85-99.
2. Kunishita, K.; Osako, T.; Tachi, Y.; Teraoka, J.; Itoh, S. Structural characterization of copper(I) complexes Supported by β-diketiminate ligands with different substitution patterns *Bull. Chem. Soc. Jpn*. **2006**, *79* 11, 1729-1741.
3. Wei N.; Murthy N. N.; Chen Q.; Zubieta, J; Karlin, K. D. Copper(I)/Dioxygen Reactivity of Mononuclear Complexes with Pyridyl and Quinolyl Tripodal Tetradentate Ligands: Reversible Formation of $Cu:O_2$ = 1:1 and 2:1 adducts. *J. Inorg. Chem*., **1994**, *33*, 1953-1965.
4. Lonnon, D. G.; Craig, D. C.; Colbran, S. B. Rhodium, palladium and platinum complexes of tris(pyridyla-lkyl)amine and tris(benzimidazolylmethyl)amine N-4-tripodal ligands. *Dalton Trans*. **2006**, 3785–3797
5. Li, J-L, *et al*. Significant differences in the biological activity of mononuclear Cu(II) and Ni(II) complexes with the polyquinolinyl ligand. *New J. Chem*. **2015**, *39*, 529-538.
6. Bulatov, E.; Haukka, M. Non-conventional synthesis and photophysical studies of platinum(II) complexes

with methylene bridged 2,2′-dipyridylamine derivatives. *Dalton Trans*. **2019**, *48*, 3369-3379.

7. Mikata, Y. *et al.* Methoxy-Substituted TQEN Family of Fluorescent Zinc Sensors. *Inorg. Chem*. **2006**, *42*, 9262-9268.
8. Mikata, Y. *et al.* Quinoline-based fluorescent zinc sensors with enhanced fluorescence intensity, Zn/Cd selectivity and metal-binding affinity by conformational restriction. *Dalton Trans*. **2013**, *42*, 9688-9698.
9. Mikata, Y.; Kizub, A.; Konno, H. TQPHEN (*N*,*N*,*N*′,*N*′-tetrakis(2-quinolylmethyl)-1,2-phenylenediamine) derivatives as highly selective fluorescent probes for $Cd^{2+}$. *Dalton Trans*. **2015**, *44*, 104-109.
10. Mikata, Y.; Kawata, K.; Iwatsuki, S.; Konno, H. Zinc-Specific Fluorescent Response of tris(isoquinolylmethyl)amines (isoTQAs). *Inorg. Chem*. **2012**, *51*, 1859-1865.
11. Ackerman, P. M.; Chipangura, M.; Mambanda, A.; Jaganyi, D. N,N-Bis(pyridin-2-ylmethyl)cyclohexanamine *Acta Cryst.* **2012**, *E68*, o2194-o2195.
12. Mambanda, A.; Jaganyi, D. A kinetics and mechanistic study on the role of the structural rigidity of the linker on the substitution reactions of chelated dinuclear Pt(II) complexes. *Dalton Trans*. **2012**, 41, 908-920.
13. Akerman, M .P.; Chiazzari, V. A. An X-ray crystallographic and DFT study of the complementary hydrogen bondi -ng of bidentate pyrrolide-imine Schiff base ligands. *J. Mol. Struct*. **2014**, *1058*, 22-30.
14. Barry, K-L.; Grimmer, C.D.; Munro, O. Q.; Akerman, M. P. Self-assembled supramolecular structures of O,N,N′ tridentate imidazole–phenol Schiff base compounds. *RSC Adv*., **2020**,*10*, 7867-7878.
15. Kohn, W. A. D.; Becke, A. D.; Parr, R. G. Density Functional Theory of Electronic Structure. *J. Phys. Chem*. **1996**, *100*, 12974-12980.
16. Bauernschmitt, R.; Ahlrichs, R. Treatment of electronic excitations within the adiabatic approximation of time dependent density functional theory. *Chem. Phys. Lett*. **1996**, 256(4): 454–464.
17. Andersson, M. P.; Uvdal, P. New Scale Factors for Harmonic Vibrational Frequencies Using the B3LYP Density Functional Method with the Triple-ζ Basis Set 6-311+G(d,p). *J. Phys. Chem. A*. **2005**, *109* (12), 2937–2941.
18. Frisch, M. J. *et al*., (2009) J. Fox, Gaussian 09, Revision E. 01, Gaussian, Inc., Wallingford CT, 2009.
19. Oxford Diffraction, CrysAlis CCD and CrysAlis RED. 2008, Oxford Diffraction Ltd, Abingdon, England.
20. Bruker, APEX2, SAINT and SADABS. 2009, Bruker AXS Inc., Madison, USA.
21. Dolomanov, O.V.; Bourhis, L.J.; Gildea, R .J.; Howard, J. A. K.; Puschmann, H. OLEX2: a complete structure solution, refinement and analysis program. *J. Appl. Cryst*. **2009**, *42*, 339-341.
22. Sheldrick, G. M. A short history of SHELX. *Acta Cryst*. 2008, *A64*, 112-122.
23. Sheldrick, G. M. Crystal structure refinement with SHELXL. *Acta Cryst*. **2015**, C71, 3-8.
24. Farrugia, L. J. WinGX and ORTEP for Windows: an update. *J. Appl. Crystallogr*. **2012**, *45*, 849-854.
25. Macrae, C. F. *et al.* Mercury CSD 2.0. *J. Appl. Crystallogr*. **2008**, *41*, 466-470.